

EMBEDDED MINIMAL DISKS

TOBIAS H. COLDING AND WILLIAM P. MINICOZZI II

Part I. The limit foliation and the singular curve

Let us start off this survey with some examples of embedded minimal disks in \mathbf{R}^3 :

Example 1: Graphs of functions $u : \Omega \rightarrow \mathbf{R}$ where $\Omega \subset \mathbf{R}^2$ is simply connected and u satisfies the minimal surface equation

$$\operatorname{div} \left(\frac{\nabla u}{\sqrt{1 + |\nabla u|^2}} \right) = 0. \tag{I.0.1}$$

Example 2: (Helicoid). See fig. 1. The minimal surface in \mathbf{R}^3 parametrized by

$$(s \cos t, s \sin t, -t) \text{ where } s, t \in \mathbf{R}. \tag{I.0.2}$$

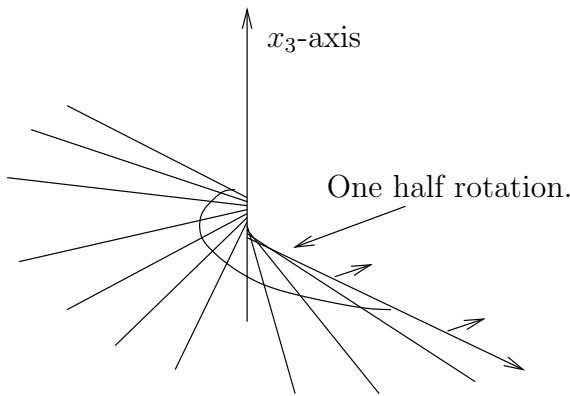


FIGURE 1. The helicoid is obtained by gluing together two ∞ -valued graphs along a line. The two multi-valued graphs are given in polar coordinates by $u_1(\rho, \theta) = -\theta$ and $u_2(\rho, \theta) = -\theta + \pi$. In either case $w(\rho, \theta) = -2\pi$.

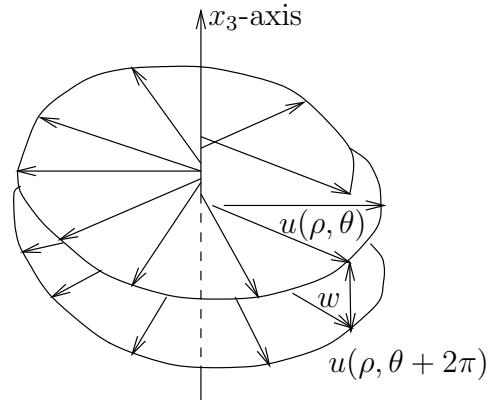


FIGURE 2. The separation of a multi-valued graph. (Here the multi-valued graph is shown with negative separation.)

One of our main theorems is that every embedded minimal disk can either be modelled by a minimal graph or by a piece of the helicoid depending on whether the curvature is small or not; see Theorem I.0.4 below.

The first author was partially supported by NSF Grant DMS 9803253 and an Alfred P. Sloan Research Fellowship and the second author by NSF Grant DMS 9803144 and an Alfred P. Sloan Research Fellowship.

To be able to discuss the helicoid some more, we will need the notion of a multi-valued graph; see fig. 2. Let D_r be the disk in the plane centered at the origin and of radius r and let \mathcal{P} be the universal cover of the punctured plane $\mathbf{C} \setminus \{0\}$ with global polar coordinates (ρ, θ) so $\rho > 0$ and $\theta \in \mathbf{R}$. An N -valued graph of a function u on the annulus $D_s \setminus D_r$ is a single valued graph over $\{(\rho, \theta) \mid r \leq \rho \leq s, |\theta| \leq N\pi\}$. The multi-valued graphs that we will consider will never close up; in fact they will all be embedded. Note that embedded corresponds to that the separation never vanishes. Here the separation (see fig. 2) is the function given by

$$w(\rho, \theta) = u(\rho, \theta + 2\pi) - u(\rho, \theta). \quad (\text{I.0.3})$$

If Σ is the helicoid, then $\Sigma \setminus x_3\text{-axis} = \Sigma_1 \cup \Sigma_2$, where Σ_1, Σ_2 are ∞ -valued graphs. Σ_1 is the graph of the function $u_1(\rho, \theta) = -\theta$ and Σ_2 is the graph of the function $u_2(\rho, \theta) = -\theta + \pi$. In either case the separation $w = -2\pi$. A multi-valued minimal graph is a multi-valued graph of a function u satisfying the minimal surface equation (I.0.1).

Here, as in [CM6] and [CM8], we have normalized so our embedded multi-valued graphs have negative separation. This can be achieved after possibly reflecting in a plane.

Using this notion of multi-valued graphs, one of our main theorems can now be stated:

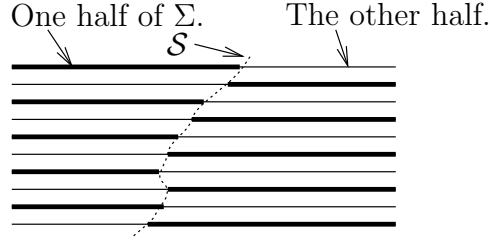


FIGURE 3. Theorem I.0.4 - the singular set, \mathcal{S} , and the two multi-valued graphs.

Theorem I.0.4. (Theorem 0.1 in [CM6]). See fig. 3. Let $\Sigma_i \subset B_{R_i} = B_{R_i}(0) \subset \mathbf{R}^3$ be a sequence of embedded minimal disks with $\partial\Sigma_i \subset \partial B_{R_i}$ where $R_i \rightarrow \infty$. If $\sup_{B_1 \cap \Sigma_i} |A|^2 \rightarrow \infty$, then there exists a subsequence, Σ_j , and a Lipschitz curve $\mathcal{S} : \mathbf{R} \rightarrow \mathbf{R}^3$ such that after a rotation of \mathbf{R}^3 :

1. $x_3(\mathcal{S}(t)) = t$. (That is, \mathcal{S} is a graph over the x_3 -axis.)
2. Each Σ_j consists of exactly two multi-valued graphs away from \mathcal{S} (which spiral together).
3. For each $1 > \alpha > 0$, $\Sigma_j \setminus \mathcal{S}$ converges in the C^α -topology to the foliation, $\mathcal{F} = \{x_3 = t\}_t$, of \mathbf{R}^3 .
4. For all $r > 0$, t , then $\sup_{B_r(\mathcal{S}(t)) \cap \Sigma_j} |A|^2 \rightarrow \infty$.

In 2., 3. that $\Sigma_j \setminus \mathcal{S}$ are multi-valued graphs and converges to \mathcal{F} means that for each compact subset $K \subset \mathbf{R}^3 \setminus \mathcal{S}$ and j sufficiently large $K \cap \Sigma_j$ consists of multi-valued graphs over (part of) $\{x_3 = 0\}$ and $K \cap \Sigma_j \rightarrow K \cap \mathcal{F}$.

Theorem I.0.4 (as many of the other results discussed below) is modelled by the helicoid and its rescalings. Take a sequence $\Sigma_i = a_i \Sigma$ of rescaled helicoids where $a_i \rightarrow 0$. The curvatures of this sequence are blowing up along the vertical axis. The sequence converges

(away from the vertical axis) to a foliation by flat parallel planes. The singular set \mathcal{S} (the axis) then consists of removable singularities.

Of the many different paths that one could choose through our results about embedded minimal disks, we have chosen here one which discusses some of our more elementary results in greater detail and then only gives a very rough overview of some of our key results which are more difficult. Our hope is that by doing so this survey can serve as a reading guide for our papers where the reader is eased into the subject and then is shown the anatomy of the proof of our main theorem.

Let x_1, x_2, x_3 be the standard coordinates on \mathbf{R}^3 . For $y \in \Sigma \subset \mathbf{R}^3$ and $s > 0$, the extrinsic and intrinsic balls are $B_s(y), \mathcal{B}_s(y)$. K_Σ the sectional curvature of a smooth compact surface Σ and when Σ is immersed A_Σ will be its second fundamental form (so when Σ is minimal, then $|A|^2 = -2K_\Sigma$). When Σ is oriented, \mathbf{n}_Σ is the unit normal.

Using Theorems I.0.4, I.3.2, W. Meeks and H. Rosenberg proved that the plane and helicoid are the only complete properly embedded simply-connected minimal surfaces in \mathbf{R}^3 , [MeRo].

I.1. MULTI-VALUED MINIMAL GRAPHS

We will later see that, just like the helicoid, general embedded minimal disks with large curvature at some interior point can be built out of multi-valued graphs. This will be particularly useful once we have a good understanding of general multi-valued minimal graphs. So let us first discuss some results about such graphs.

In [CM3] we showed (essentially by a gradient estimate) that the separation between the sheets grows sublinearly (in Theorem I.1.3 below we will discuss an improvement of this when the number of sheets grows sufficiently fast). Precisely, in proposition II.2.12 of [CM3] we showed that given $\alpha > 0$, there exists N_g so if Σ is an N_g -valued minimal graph over $D_{e^{N_g}R} \setminus D_{e^{-N_g}R}$ of u and $w < 0$, then

$$\rho |\text{Hess}_u| + \rho |\nabla w|/|w| \leq \alpha \text{ on } \{1 \leq \rho \leq R \text{ and } |\theta| \leq \pi\}. \quad (\text{I.1.1})$$

In particular, by integrating, the separation grows at most like ρ^α . Thus, choosing $\alpha < 1$, it follows that the growth is sublinear.

Using that the Gauss map is conformal, we showed in corollary 2.3 of [CM8] that the curvature of a 2-valued embedded minimal graph decays faster than quadratically, i.e., we showed that

$$|A|^2 \leq C r^{-2-5/6} \quad (\text{I.1.2})$$

for embedded 2-valued minimal graphs whose separation grows sublinearly; cf. (I.1.1). (Note that by [CM3], there exists N_g so this applies to any N_g -valued embedded minimal graph.) The important point for the applications in [CM8] is that the faster than linear decay on the Hessian of u that (I.1.2) implies together with the form of (I.0.1) gives that $|\Delta u|$ decays faster than quadratically; see equation (3.6) in [CM8].

The above bound (I.1.2) used the nonlinearity of the minimal surface equation much like the nonlinearity is needed for proving the Bernstein theorem. In other situations the nonlinearity seems more to add difficulties than being of any help. In those situations one tries to model the minimal surface equation by the Laplace equation and use that from (I.1.2) if u is a multi-valued solution of the minimal surface equation, then $|\Delta u|$ decays faster than quadratically so that u “become more and more like a harmonic function”. We will now take

advantage of this to discuss some analysis of such multi-valued solutions that we will need later. This analysis is from [CM8].

The first such result is the following sharp upper and lower bound for the separation of a multi-valued graph:

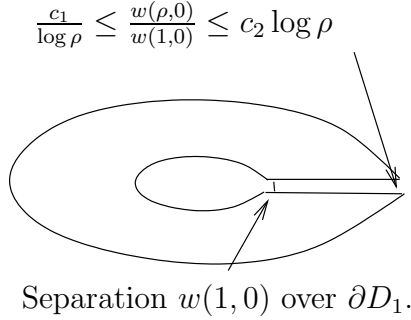


FIGURE 4. Theorem I.1.3: The sharp logarithmic upper and lower bounds for the separation.

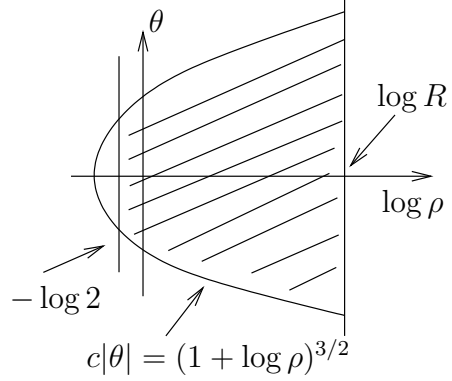


FIGURE 5. The domain of u in Theorem I.1.3 in $(\log \rho, \theta)$ -coordinates.

Theorem I.1.3. (Theorem 1.3 of [CM8]). See fig. 4 and fig. 5. Given $c > 0$, there exists c_1, c_2 such that if u satisfies (I.0.1) on $\{(\rho, \theta) \mid 1/2 \leq \rho \leq R \text{ and } c|\theta| \leq (1 + \log \rho)^{3/2}\}$ and $w < 0$ together with a slight condition on the growth of u and w (see equation (1.5) in [CM8]), then for $2 \leq \rho \leq R^{1/2}$

$$\frac{c_1}{\log \rho} \leq \frac{w(\rho, 0)}{w(1, 0)} \leq c_2 \log \rho. \quad (\text{I.1.4})$$

The idea of the lower bound for the separation, i.e., $w(\rho, 0)/w(1, 0) \geq c_1/\log \rho$: If u is as in Theorem I.1.3, then $w < 0$ is almost harmonic and it can be seen to follow from (I.1.2) and the form of (I.0.1) that so is $\tilde{w}(x, y) = w(e^x, y)$. Moreover, $\tilde{w} < 0$ is defined on a domain that is conformally close to a half-disk (see lemma 3.2 of [CM8]). Suppose for a moment that \tilde{w} was actually harmonic and defined on the half-space $\{x > -\log 2\}$, then by the mean value equality (see fig. 6) and the sign on \tilde{w}

$$w(e^x, 0) = \tilde{w}(x, 0) = \frac{1}{2\pi x} \int_{\partial D_x(x, 0)} \tilde{w} \leq \frac{1}{2\pi x} \int_{D_1 \cap \partial D_x(x, 0)} \tilde{w}. \quad (\text{I.1.5})$$

By the Harnack inequality, it would then follow from (I.1.5) that $w(e^x, 0) = \tilde{w}(x, 0) \leq c_1 \tilde{w}(0, 0)/x$; which is the desired lower bound. The upper bound follows similarly or by an inversion formula; see section 3 of [CM8].

By Theorem I.1.3, the fastest possible decay for $w(\rho, 0)/w(1, 0)$ is $c_1/\log \rho$. Hence if $\tilde{w}(x + iy) = w(e^x, y)$, then the fastest possible decay for $\tilde{w}(x, 0)/\tilde{w}(0, 0)$ is c_1/x and as mentioned above, then using (I.1.2) it can be seen that \tilde{w} is almost harmonic. This decay is achieved for the harmonic function $\tilde{v}(z) = -\text{Re } z^{-1} = -x/(x^2 + y^2) < 0$ (see fig. 7) and if

$$u(\rho, \theta) = \int_0^\theta v(\rho, y) dy = \int_0^\theta \tilde{v}(\log \rho, y) dy = \int_0^\theta \frac{-\log \rho dy}{(\log \rho)^2 + y^2} = -\arctan \frac{\theta}{\log \rho}, \quad (\text{I.1.6})$$

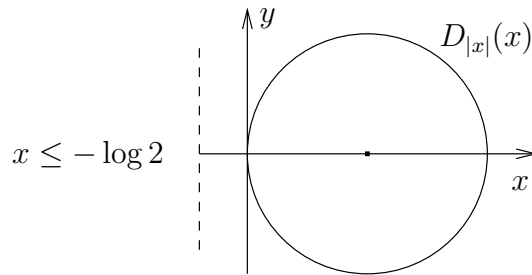


FIGURE 6. Proof of Theorem I.1.3: Applying the mean value equality to a negative harmonic function defined in a half-space.

then the graph of u is an embedded ∞ -valued harmonic graph lying in a slab, i.e., $|u| \leq \pi/2$, and hence in particular is not proper. Note also that if u is given by (I.1.6), then $u_\theta = v$ and w/v is uniformly bounded above and below. We next want to rule out not only this as an example of one half of an embedded minimal disk, but more generally any ∞ -valued minimal graph in a half-space.

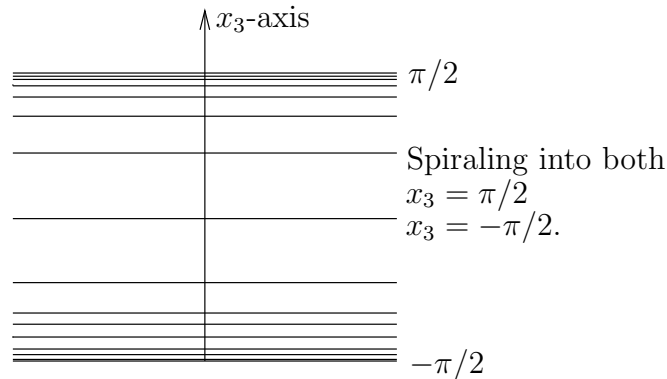


FIGURE 7. Properness; e.g., need to rule out that one of the multi-valued graphs can contain a graph like $\arctan(\theta/\log \rho)$, where (ρ, θ) are polar coordinates.

I.2. TOWARDS REMOVABILITY OF SINGULARITIES

As mentioned above, we next want to rule out that any ∞ -valued graph which lies in a half-space can be one half of an embedded minimal disk. This is done in Theorem I.2.1 below where the short curves σ_θ in the minimal disk will connect two multi-valued sub-graphs and thus each sub-graph is essentially one half of the disk. These curves are needed to conclude properness since, as mentioned above, just having one ∞ -valued minimal graph in a slab is not in itself a contradiction.

Let us illustrate in an example how these curves σ could be chosen. If Σ is the helicoid (here, to be consistent with [CM8], we use the helicoid which spirals downward so $w < 0$), i.e., $\Sigma = (s \cos t, s \sin t, -t)$ where $s, t \in \mathbf{R}$, then $\Sigma \setminus \{s = 0\}$ consists of two ∞ -valued graphs Σ_1, Σ_2 and the curves $\sigma_t = \Sigma \cap \{x_3 = t\}$ are short curves connecting the two halves; see fig. 8.

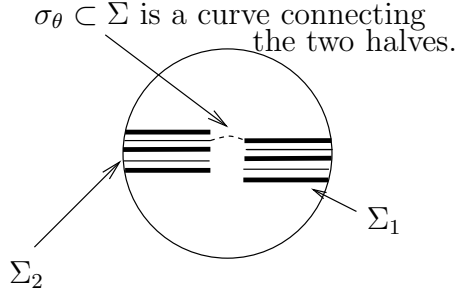


FIGURE 8. The short curves σ_θ in Theorem I.2.1 connecting the two multi-valued graphs.

Theorem I.2.1. (See corollary 1.2 in [CM8] for the precise statement). Let Σ_i be a sequence as in Theorem I.0.4 and suppose that $\Sigma_{i,1}, \Sigma_{i,2}$ are multi-valued graphs in Σ_i that spiral together (one inside the other). We claim that if $\Sigma_{i,1}, \Sigma_{i,2}$ can be connected by short curves in Σ_i (see fig. 8), then they cannot spiral into a plane. That is, they cannot accumulate in finite height.

The idea of the proof of Theorem I.2.1: Let Σ_1, Σ_2 be two ∞ -valued graphs of u_1, u_2 that spiral together, are part of an embedded minimal disk, and can be connected by short curves in the disk. We claim that the two graphs must grow out of any half-space. Suppose that they are contained in the half-space $u_i \geq 0$ and that they spiral downward, i.e., $w_i < 0$; we will get a contradiction.

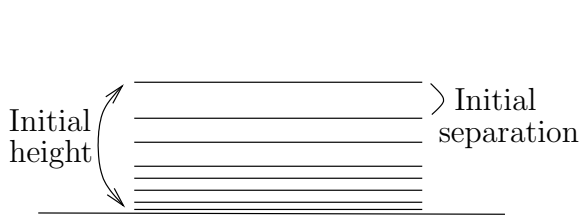


FIGURE 9. The flux argument in the proof of Theorem I.2.1: The initial height and separation.

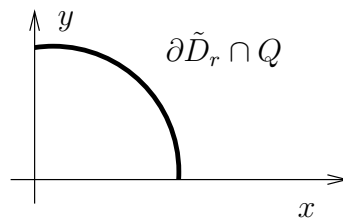


FIGURE 10. The flux argument in the proof of Theorem I.2.1: The curve where the average is calculated over.

Using that the curvature of a multi-valued embedded minimal graph decays faster than quadratically will allow us (as in Theorem I.1.3) to model the graphs Σ_1, Σ_2 by graphs of harmonic functions. So suppose for a moment that both u_1 and u_2 are harmonic. We will show, using a flux argument, that if the separation is large compared with the initial height

(see fig. 9), then the fact that the two graphs are part of an embedded minimal disk will eventually force the graphs to grow out of the half-space that they are assumed to lie in. Namely, set $\tilde{u}_i(x, y) = u_i(e^x, y)$ (i.e., $\rho = e^x$ and $\theta = y$) and let Q be the quarter-space $\{(x, y) \mid x, y \geq 0\}$ and $\tilde{D}_r = \{(x, y) \mid x^2 + y^2 \leq r^2\}$. To see that each of the two graphs would grow out of the half-space, set (see fig. 10)

$$Av_i(r) = \frac{1}{r} \int_{\partial \tilde{D}_r \cap Q} \tilde{u}_i. \quad (\text{I.2.2})$$

The claim follows once we show that there are constants C_1 and C_2 depending on the ratio of the initial height with the initial separation so that for $r \geq 2$

$$Av_1(r) + Av_2(r) - Av_1(1) - Av_2(1) \leq -C_1 \log^2 r + C_2 \log r. \quad (\text{I.2.3})$$

Namely, note that if (I.2.3) holds, then the left hand side of (I.2.3) goes to negative infinity. To see (I.2.3), note that when u_i is harmonic, then so is \tilde{u}_i and by Stokes' theorem

$$Av'_i(r) = \frac{1}{r} \int_{\partial \tilde{D}_r \cap Q} \frac{d\tilde{u}_i}{dn} = \frac{1}{r} \int_0^r \frac{\partial \tilde{u}_i}{\partial y}(s, 0) ds + \frac{1}{r} \int_0^r \frac{\partial \tilde{u}_i}{\partial x}(0, s) ds. \quad (\text{I.2.4})$$

Using that the separation is roughly equal to $2\pi(u_i)_\theta$ we get by combining (I.2.4) with the lower bound for the separation from Theorem I.1.3 that (more or less)

$$Av'_i(r) \leq -\frac{C_1 \log r}{2r} + \frac{1}{r} \int_0^r \frac{\partial \tilde{u}_i}{\partial x}(0, s) ds. \quad (\text{I.2.5})$$

Adding Av'_1 and Av'_2 and using that the two spiralling curves (i.e., $\theta \rightarrow (\theta, u_i(1, \theta))$ for $i = 1, 2$, see fig. 11) together with the two short curves that are assumed to exist bounds a disk (see fig. 12) we get by Stokes' theorem (see lemma 5.1 of [CM8]) that

$$Av'_1(r) + Av'_2(r) \leq -\frac{C_1 \log r}{2r} + \frac{C_2}{r}. \quad (\text{I.2.6})$$

Integrating (I.2.6) gives (I.2.3).

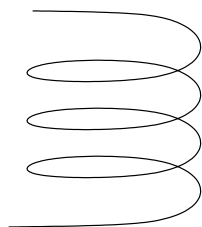


FIGURE 11. The flux argument in the proof of Theorem I.2.1: One of the two spiralling curves; $\theta \rightarrow (\theta, u_i(1, \theta))$.

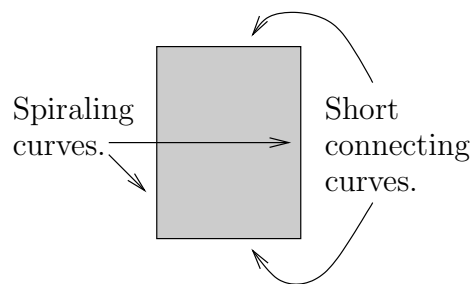


FIGURE 12. The flux argument in the proof of Theorem I.2.1: The two short curves together with the two spiralling curves bounds a disk in Σ .

In the general case where u_i satisfies the minimal surface equation there are a number of difficulties that have to be dealt with; see lemma 4.1 of [CM8].

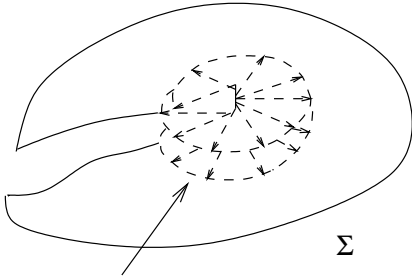
Now this was a little analysis of multi-valued solutions of the minimal surface equation and can all be found in [CM8]. It illustrates that once we show existence of multi-valued

minimal graphs in embedded minimal disks and know that such graphs extend as graphs with a sufficiently rapidly growing number of sheets, then we get a removable singularity theorem.

I.3. EXISTENCE OF MULTI-VALUED GRAPHS AND THE ONE-SIDED CURVATURE ESTIMATE

We now come to our key results for embedded minimal disks. The first says that if the curvature of such a disk Σ is large at some point $x \in \Sigma$, then nearby x a multi-valued graph forms (in Σ) and this extends (in Σ) almost all the way to the boundary. Precisely this is:

Theorem I.3.1. (Theorem 0.2 in [CM4]). See fig. 13 and fig. 14. Given $N \in \mathbf{Z}_+$, $\epsilon > 0$, there exist $C_1, C_2 > 0$ so: Let $0 \in \Sigma \subset B_R \subset \mathbf{R}^3$ be an embedded minimal disk, $\partial\Sigma \subset \partial B_R$. If $\max_{B_{r_0} \cap \Sigma} |A|^2 \geq 4C_1^2 r_0^{-2}$ for some $R > r_0 > 0$, then there exists (after a rotation) an N -valued graph $\Sigma_g \subset \Sigma$ over $D_{R/C_2} \setminus D_{2r_0}$ with gradient $\leq \epsilon$ and $\Sigma_g \subset \{x_3^2 \leq \epsilon^2(x_1^2 + x_2^2)\}$.



Small multi-valued graph near 0.

FIGURE 13. Part 1 of the proof of Theorem I.3.1; see Theorem II.0.13 - finding a small multi-valued graph in a disk near a point of large curvature.

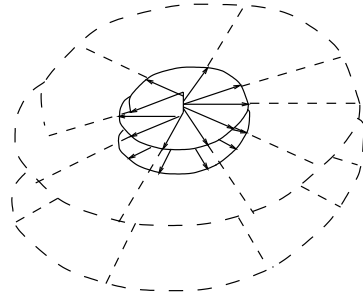


FIGURE 14. Part 2 of the proof of Theorem I.3.1; see Theorem II.0.15 - extending a small multi-valued graph in a disk.

As a consequence of Theorem I.3.1, one easily gets that if $|A|^2$ is blowing up near 0 for a sequence of embedded minimal disks Σ_i , then there is a sequence of 2-valued graphs $\Sigma_{i,d} \subset \Sigma_i$, where the 2-valued graphs start off on a smaller and smaller scale (namely, r_0 in Theorem I.3.1 can be taken to be smaller as the curvature gets larger). Consequently, by the sublinear separation growth, such 2-valued graphs collapse and, hence, a subsequence converges to a smooth minimal graph through 0. (Here 0 is a removable singularity for the limit.) Moreover, if the sequence of such disks is as in Theorem I.0.4, i.e., if $R_i \rightarrow \infty$, then the minimal graph in the limit is entire and hence, by Bernstein's theorem, is a plane.

The second key result is the following curvature estimate for embedded minimal disks in a half-space:

Theorem I.3.2. (Theorem 0.2 in [CM6]). See fig. 15. There exists $\epsilon > 0$, such that if $\Sigma \subset B_{2r_0} \cap \{x_3 > 0\} \subset \mathbf{R}^3$ is an embedded minimal disk with $\partial\Sigma \subset \partial B_{2r_0}$, then for all components Σ' of $B_{r_0} \cap \Sigma$ which intersect $B_{\epsilon r_0}$

$$\sup_{\Sigma'} |A_{\Sigma}|^2 \leq r_0^{-2}. \quad (\text{I.3.3})$$

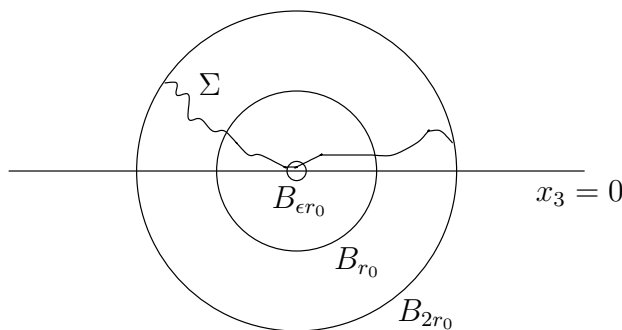


FIGURE 15. Theorem I.3.2 - the one-sided curvature estimate for an embedded minimal disk Σ in a half-space with $\partial\Sigma \subset \partial B_{2r_0}$: The components of $B_{r_0} \cap \Sigma$ intersecting $B_{\epsilon r_0}$ are graphs.

Using the minimal surface equation and that Σ' has points close to a plane, it is not hard to see that, for $\epsilon > 0$ sufficiently small, (I.3.3) is equivalent to the statement that Σ' is a graph over the plane $\{x_3 = 0\}$.

An embedded minimal surface Σ which is as in Theorem I.3.2 is said to satisfy the (ϵ, r_0) -effective one-sided Reifenberg condition; cf. appendix A of [CM6] and the appendix of [ChC]. We will often refer to Theorem I.3.2 as *the one-sided curvature estimate*.

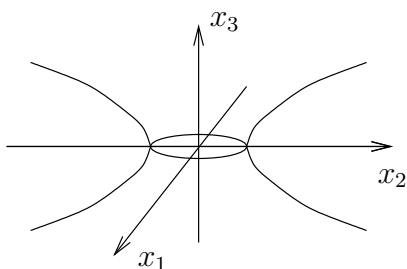


FIGURE 16. The catenoid given by revolving $x_1 = \cosh x_3$ around the x_3 -axis.

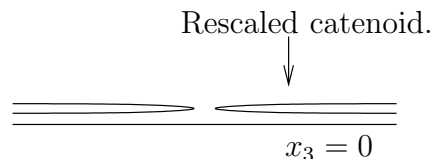


FIGURE 17. Rescaling the catenoid shows that simply connected is needed in the one-sided curvature estimate.

Note that the assumption in Theorem I.3.2 that Σ is simply connected is crucial as can be seen from the example of a rescaled catenoid. The catenoid is the minimal surface in \mathbf{R}^3 given by $(\cosh s \cos t, \cosh s \sin t, s)$ where $s, t \in \mathbf{R}$; see fig. 16. Under rescalings this converges (with multiplicity two) to the flat plane; see fig. 17. Likewise, by considering the universal cover of the catenoid, one sees that embedded, and not just immersed, is needed in Theorem I.3.2.

An almost immediate consequence of Theorem I.3.2 is:

Corollary I.3.4. (Corollary 0.4 in [CM6]). See fig. 18. There exist $c > 1$, $\epsilon > 0$ so: Let $\Sigma_1, \Sigma_2 \subset B_{cr_0} \subset \mathbf{R}^3$ be disjoint embedded minimal surfaces with $\partial\Sigma_i \subset \partial B_{cr_0}$ and

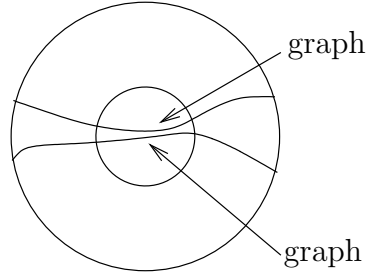


FIGURE 18. Corollary I.3.4: Two sufficiently close components of an embedded minimal disk must each be a graph.

$B_{\epsilon r_0} \cap \Sigma_i \neq \emptyset$. If Σ_1 is a disk, then for all components Σ'_1 of $B_{r_0} \cap \Sigma_1$ which intersect $B_{\epsilon r_0}$

$$\sup_{\Sigma'_1} |A|^2 \leq r_0^{-2}. \quad (\text{I.3.5})$$

If $\delta > 0$ and $z \in \mathbf{R}^3$, then we denote by $\mathbf{C}_\delta(z)$ the (convex) cone with vertex z , cone angle $(\pi/2 - \arctan \delta)$, and axis parallel to the x_3 -axis. That is, see fig. 21,

$$\mathbf{C}_\delta(z) = \{x \in \mathbf{R}^3 \mid x_3^2 \geq \delta^2 (x_1^2 + x_2^2)\} + z. \quad (\text{I.3.6})$$

In the proof of Theorem I.0.4, the following (direct) consequence of Theorem I.3.2 with Σ_d playing the role of the plane is needed:

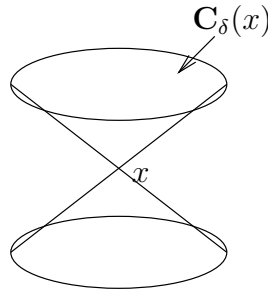


FIGURE 19. The cone $\mathbf{C}_\delta(x)$.

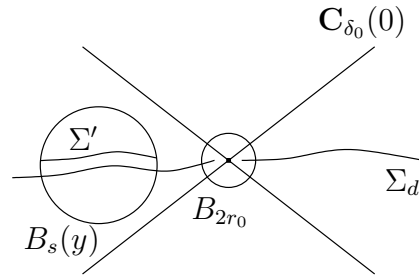


FIGURE 20. Corollary I.3.7: With Σ_d playing the role of $x_3 = 0$, by the one-sided estimate, Σ consists of multi-valued graphs away from a cone.

Corollary I.3.7. (Corollary I.1.9 in [CM6]). See fig. 20. There exists $\delta_0 > 0$ so: Suppose $\Sigma \subset B_{2R}$, $\partial\Sigma \subset \partial B_{2R}$ is an embedded minimal disk containing a 2-valued graph $\Sigma_d \subset \{x_3^2 \leq \delta_0^2 (x_1^2 + x_2^2)\}$ over $D_R \setminus D_{r_0}$ with gradient $\leq \delta_0$. Then each component of $B_{R/2} \cap \Sigma \setminus (\mathbf{C}_{\delta_0}(0) \cup B_{2r_0})$ is a multi-valued graph with gradient ≤ 1 .

Note that, since Σ is compact and embedded, the multi-valued graphs given by Corollary I.3.7 spiral through the cone. Namely, if a graph did close up, then the graph containing Σ_d would be forced to accumulate into it, contradicting compactness.

It can also be seen from Corollary I.3.7 (see corollary 6.3 of [CM8]) that if Σ_d and Σ are as in Corollary I.3.7, then Σ_d extends in $\Sigma \setminus \mathbf{C}_{\delta_0}(0)$ to a multi-valued graph with at least $(\log \rho)^2$ many sheets. Thus Theorem I.1.3 applies.

I.4. REGULARITY OF THE SINGULAR SET AND THEOREM I.0.4

Next we will see, by a very general compactness argument, that for any sequence of surfaces in \mathbf{R}^3 (minimal or not), after possibly going to a subsequence, then there is a well defined notion of points where the second fundamental form of the sequence blows up.

Lemma I.4.1. Let $\Sigma_i \subset B_{R_i}$, $\partial\Sigma_i \subset \partial B_{R_i}$, and $R_i \rightarrow \infty$ be a sequence of (smooth) compact surfaces. After passing to a subsequence, Σ_j , we may assume that for each $x \in \mathbf{R}^3$ either (a) or (b) holds:

- (a) $\sup_{B_r(x) \cap \Sigma_j} |A|^2 \rightarrow \infty$ for all $r > 0$,
- (b) $\sup_j \sup_{B_r(x) \cap \Sigma_j} |A|^2 < \infty$ for some $r > 0$.

Proof. For $r > 0$ and an integer n , define a sequence of functions on \mathbf{R}^3 by

$$\mathcal{A}_{i,r,n}(x) = \min\{n, \sup_{B_r(x) \cap \Sigma_i} |A|^2\}, \quad (\text{I.4.2})$$

where we set $\sup_{B_r(x) \cap \Sigma_i} |A|^2 = 0$ if $B_r(x) \cap \Sigma_i = \emptyset$. Set

$$\mathcal{D}_{i,r,n} = \lim_{k \rightarrow \infty} 2^{-k} \sum_{m=0}^{2^k-1} \mathcal{A}_{i,(1+m2^{-k})r,n}, \quad (\text{I.4.3})$$

then $\mathcal{D}_{i,r,n}$ is continuous and $\mathcal{A}_{i,2r,n} \geq \mathcal{D}_{i,r,n} \geq \mathcal{A}_{i,r,n}$. Let $\nu_{i,r,n}$ be the (bounded) functionals,

$$\nu_{i,r,n}(\phi) = \int_{B_n} \phi \mathcal{D}_{i,r,n} \text{ for } \phi \in L^2(\mathbf{R}^3). \quad (\text{I.4.4})$$

By standard compactness for fixed r, n , after passing to a subsequence, $\nu_{j,r,n} \rightarrow \nu_{r,n}$ weakly. In fact (since the unit ball in $L^2(\mathbf{R}^3)$ has a countable basis), by an easy diagonal argument, after passing to a subsequence, we may assume that for all $n, m \geq 1$ fixed $\nu_{j,2^{-m}n} \rightarrow \nu_{2^{-m}n}$ weakly. Note that if $x \in \mathbf{R}^3$ and for all m, n with $n \geq |x| + 1$, (identify $B_{2^{-m}}(x)$ with its characteristic function)

$$\nu_{2^{-m}n}(B_{2^{-m}}(x)) \geq n \text{Vol}(B_{2^{-m}}), \quad (\text{I.4.5})$$

then for each fixed $r > 0$, $\sup_{B_r(x) \cap \Sigma_j} |A|^2 \rightarrow \infty$. Conversely, if for some $n \geq |x| + 1$, m , (I.4.5) fails at x , then $\sup_j \sup_{B_r(x) \cap \Sigma_j} |A|^2 < \infty$ for $r = 2^{-m-1}$. \square

Fix $\delta > 0$. We will say that a subset $\mathcal{S} \subset \mathbf{R}^3$ has the cone property (or the δ -cone property) if \mathcal{S} is closed and nonempty and the following holds:

- (1) If $z \in \mathcal{S}$, then $\mathcal{S} \subset \mathbf{C}_\delta(z)$.
- (2) If $t \in x_3(\mathcal{S})$ and $\epsilon > 0$, then $\mathcal{S} \cap \{t < x_3 < t + \epsilon\} \neq \emptyset$ and $\mathcal{S} \cap \{t - \epsilon < x_3 < t\} \neq \emptyset$.

Note that (2) just says that each point in \mathcal{S} is the limit of points coming from above and below.

When $\Sigma_i \subset B_{R_i} \subset \mathbf{R}^3$ is a sequence of embedded minimal disks with $\partial\Sigma_i \subset \partial B_{R_i}$, $R_i \rightarrow \infty$ and Σ_j is the subsequence given by Lemma I.4.1 and \mathcal{S} is the sets of points where the curvatures of Σ_j blow up (i.e., where (a) in Lemma I.4.1 holds), then we will see below that

\mathcal{S} has the cone property (after a rotation of \mathbf{R}^3). Hence (by the next lemma), \mathcal{S} is in this case a Lipschitz curve which is a graph over the x_3 -axis. Note that in the case where Σ_i is a sequence of rescaled helicoids, then \mathcal{S} is the x_3 -axis.

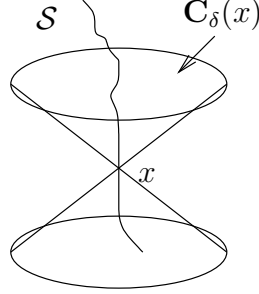


FIGURE 21. It follows from the one-sided curvature estimate that the singular set has the cone property and hence is a Lipschitz curve.

Lemma I.4.6. See fig. 21. If $\mathcal{S} \subset \mathbf{R}^3$ has the δ -cone property, then $\mathcal{S} \cap \{x_3 = t\}$ consists of exactly one point \mathcal{S}_t for all $t \in \mathbf{R}$, and $t \rightarrow \mathcal{S}_t$ is a Lipschitz parameterization of \mathcal{S} with

$$|t_2 - t_1| \leq |\mathcal{S}_{t_2} - \mathcal{S}_{t_1}| \leq \sqrt{1 + \delta^{-2}} |t_2 - t_1|. \quad (\text{I.4.7})$$

Proof. Since \mathcal{S} is nonempty, we may after translation assume that $0 \in \mathcal{S}$. By (1), it follows that $\mathcal{S} \cap \{x_3 = t\}$ consists of at most one point for each $t \in \mathbf{R}$. Assume that $\mathcal{S} \cap \{x_3 = t_0\} = \emptyset$ for some t_0 . Since $\mathcal{S} \subset \mathbf{R}^3$ is a nonempty closed set and $x_3 : \mathcal{S} \subset \mathbf{C}_\delta(0) \rightarrow \mathbf{R}$ is proper, then $x_3(\mathcal{S}) \subset \mathbf{R}$ is also closed (and nonempty). Let $t_s \in x_3(\mathcal{S})$ be the closest point in $x_3(\mathcal{S})$ to t_0 . The desired contradiction now easily follows since either $\mathcal{S} \cap \{t_s < x_3 < t_0\}$ or $\mathcal{S} \cap \{t_0 < x_3 < t_s\}$ is nonempty by assumption.

It follows that $t \rightarrow \mathcal{S}_t$ is a well-defined curve (from \mathbf{R} to \mathcal{S}). Moreover, since $\mathcal{S}_{t_2} \subset \{x_3 = t_1 + (t_2 - t_1)\} \cap \mathbf{C}_\delta(\mathcal{S}_{t_1}) \subset B_{\sqrt{1+\delta^{-2}}|t_2-t_1|}(\mathcal{S}_{t_1})$, (I.4.7) follows. \square

Suppose next that Σ_i is as in Theorem I.0.4 and Σ_j, \mathcal{S} are given by Lemma I.4.1, then \mathcal{S} is closed by definition and nonempty by the assumption of Theorem I.0.4. From Corollary I.3.7 (cf. the sketch of the proof of Theorem I.0.4 below), it follows that (1) above holds, so to see that \mathcal{S} has the cone property all we need to see is that (2) holds. This follows from the next lemma which relies in part on Theorem I.2.1:

Lemma I.4.8. (Lemma I.1.10 in [CM6]). See fig. 22. There exists $c_0 > 0$ so: Let $\Sigma_i \subset B_{R_i}$, $\partial\Sigma_i \subset \partial B_{R_i}$ be a sequence of embedded minimal disks with $R_i \rightarrow \infty$. If $\Sigma_{d,i} \subset \Sigma_i$ is a sequence of 2-valued graphs over $D_{R_i/C} \setminus D_{\epsilon_i}$ with $\epsilon_i \rightarrow 0$ and $\Sigma_{d,i} \rightarrow \{x_3 = 0\} \setminus \{0\}$, then

$$\sup_{B_1 \cap \Sigma_i \cap \{x_3 > c_0\}} |A|^2 \rightarrow \infty. \quad (\text{I.4.9})$$

Sketch of the proof of Theorem I.0.4: From all of these results above, we know that if Σ_i is a sequence as in Theorem I.0.4 and Σ_j, \mathcal{S} are given by Lemma I.4.1, then \mathcal{S} has the cone property and hence, by Lemma I.4.1, \mathcal{S} is a Lipschitz graph over the x_3 -axis. As mentioned above, it also follows from Theorem I.3.1 together with Bernstein's theorem that, for each

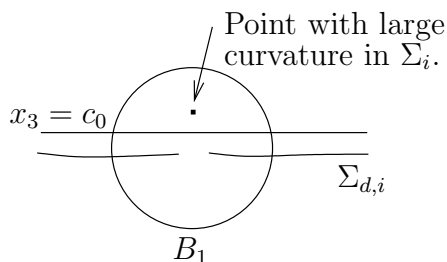


FIGURE 22. Lemma I.4.8 - points with large curvature in Σ_i above the plane $x_3 = c_0$ but near the center of the 2-valued graphs $\Sigma_{d,i}$.

$x \in \mathcal{S}$ and each j sufficiently large, there is a 2-valued graph in Σ_j and that this sequence of 2-valued graphs converges (after possibly going to a subsequence) to a plane through x . Since Σ_j is embedded, all of these planes coming from different $x \in \mathcal{S}$ must be parallel and it now follows from the one sided curvature estimate that Σ_j consists of multi-valued graphs away from \mathcal{S} . It is easy to see that there must be at least two such multi-valued graphs in the complement of \mathcal{S} . That there are not more than two follows from a barrier argument; see proposition II.1.3 of [CM6]. This is a rough sketch of the proof of Theorem I.0.4.

Part II. The proof of the existence of multi-valued graphs

To describe the existence of multi-valued graphs in embedded minimal disks, we will need the notion of a blow up point.

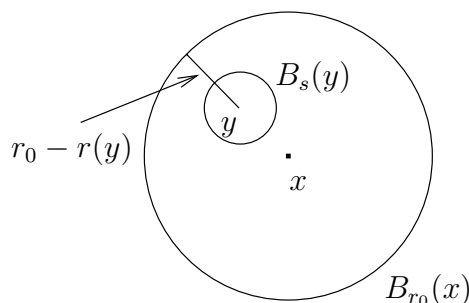


FIGURE 23. Existence of blowup points, that is pairs of points $y \in \Sigma$ and $s > 0$ satisfying (II.0.10).

Let $x \in \Sigma \subset B_{r_0}(x) \subset \mathbf{R}^3$ be a smooth (compact) surface embedded, or just immersed, with $\partial\Sigma \subset \partial B_{r_0}(x)$. Here $B_{r_0}(x)$ is the extrinsic ball of radius r_0 but could as well have been an intrinsic ball in which case the notion of a blow up point below would have to be appropriately changed. Suppose that $|A|^2(x) \geq 4C^2 r_0^{-2}$ for some constant $C > 0$. We claim that there is $y \in B_{r_0}(x) \cap \Sigma$ and $s > 0$ such that $B_s(y) \subset B_{r_0}(x)$ and

$$\sup_{B_s(y) \cap \Sigma} |A|^2 \leq 4C^2 s^{-2} = 4|A|^2(y). \quad (\text{II.0.10})$$

That is, the curvature at y is large (this just means that C should be thought of as a large constant) and is almost (up to the constant 4) the maximum on the ball $B_s(y)$. That there exists such a point y is easy to see; on $B_{r_0}(x) \cap \Sigma$ set $F(z) = (r_0 - r(z))^2 |A|^2(z)$ where $r(z) = |z - x|$. Then

$$F(x) \geq 4C^2, F \geq 0, \text{ and } F|_{\partial B_{r_0}(x) \cap \Sigma} = 0. \quad (\text{II.0.11})$$

Let y be where the maximum of F is achieved and set $s = C/|A|(y)$. One easily checks that y, s have the required properties; see fig. 23. Namely, clearly $|A|^2(y) = C^2 s^{-2}$ and since y is where the maximum of F is achieved,

$$|A|^2(z) \leq \left(\frac{r_0 - r(y)}{r_0 - r(z)} \right)^2 |A|^2(y). \quad (\text{II.0.12})$$

Since $F(x) \geq 4C^2$ it follows from the choice of s that $|r_0 - r(y)| \leq 2|r_0 - r(z)|$ for $z \in B_s(y) \cap \Sigma$. Hence, $|A|^2(z) \leq 4|A|^2(y)$. Together this gives (II.0.10).

Returning to the existence of multi-valued graphs, then the way we showed Theorem I.3.1 was by combining a blow up result with [CM3]. This blow up result says that if an embedded minimal disk in a ball has large curvature at a point, then it contains a small (in fact on the scale of one over the square root of the curvature) almost flat multi-valued graph nearby, that is:

Theorem II.0.13. (Theorem 0.4 in [CM4]). See fig. 13. Given $N, \omega > 1$, and $\epsilon > 0$, there exists $C = C(N, \omega, \epsilon) > 0$ so: Let $0 \in \Sigma \subset B_R \subset \mathbf{R}^3$ be an embedded minimal disk, $\partial \Sigma \subset \partial B_R$. If $\sup_{B_{r_0} \cap \Sigma} |A|^2 \leq 4C^2 r_0^{-2} = 4|A|^2(0)$ for some $0 < r_0 < R$, then there exist $\bar{R} < r_0/\omega$ and (after a rotation) an N -valued graph $\Sigma_g \subset \Sigma$ over $D_{\omega \bar{R}} \setminus D_{\bar{R}}$ with gradient $\leq \epsilon$, and $\text{dist}_{\Sigma}(0, \Sigma_g) \leq 4\bar{R}$.

Note that 0 in Theorem II.0.13 is a blow up point in the above sense.

The result that we needed from [CM3] (combining theorem 0.3 and lemma II.3.8 there) is Theorem II.0.15 below that allows us to extend the (small) multi-valued graphs given by Theorem II.0.13 almost out to the boundary of the ‘‘big’’ ball B_R . In this theorem by the middle sheet $(\Sigma_g)^M$ of an N -valued graph Σ_g we mean the portion over

$$\{(\rho, \theta) \in \mathcal{P} \mid r_1 < \rho < r_2 \text{ and } 0 \leq \theta \leq 2\pi\}. \quad (\text{II.0.14})$$

Theorem II.0.15. [CM3]. See fig. 14. Given N_1 and $\tau > 0$, there exist $N, \Omega, \epsilon > 0$ so: If $\Omega r_0 < 1 < R/\Omega$, $\Sigma \subset B_R$ is an embedded minimal disk with $\partial \Sigma \subset \partial B_R$, and Σ contains an N -valued minimal graph Σ_g over $D_1 \setminus D_{r_0}$ with gradient $\leq \epsilon$ and $\Sigma_g \subset \{x_3^2 \leq \epsilon^2(x_1^2 + x_2^2)\}$, then Σ contains a N_1 -valued graph Σ_d over $D_{R/\Omega} \setminus D_{r_0}$ with gradient $\leq \tau$ and $(\Sigma_g)^M \subset \Sigma_d$.

II.1. THE PROOF OF THEOREM II.0.13

We will here describe some of the ideas that go into the proof of Theorem II.0.13. Roughly, we use the upper bound on $|A|^2$ to bound the area growth of intrinsic balls and, consequently, get an average curvature bound. We then use this to find large pieces of Σ with an improved (quadratic) curvature bound. Using the lower bound on $|A|^2(0)$, we show that there are many such pieces so that two must be close; embeddedness implies that these are disjoint, hence almost stable, and therefore nearly flat. These large flat pieces then give the desired N -valued graph.

Throughout this section, $\Sigma \subset B_R$ is an embedded minimal disk with $\partial\Sigma \subset \partial B_R$.

Area and total curvature. As in corollary 1.7 of [CM4], integrating the Jacobi equation and using $K_\Sigma = -|A|^2/2$ gives

$$4(\text{Area}(\mathcal{B}_R) - \pi R^2) = 2 \int_0^R \int_0^t \int_{\mathcal{B}_s} |A|^2 = \int_{\mathcal{B}_R} |A|^2 (R-r)^2. \quad (\text{II.1.1})$$

The second equality used two integrations by parts (i.e., $\int_0^R f(t) g''(t) dt$ with $f(t) = \int_0^t \int_{\mathcal{B}_s} |A|^2$ and $g(t) = (R-t)^2$). We will see that (II.1.1) leads to area bounds. For example, when \mathcal{B}_R is stable, then using $R-r$ (where $r(x) = \text{dist}_\Sigma(0, x)$) in the stability inequality gives

$$4(\text{Area}(\mathcal{B}_R) - \pi R^2) = \int_{\mathcal{B}_R} |A|^2 (R-r)^2 \leq \int_{\mathcal{B}_R} |\nabla(R-r)|^2 = \text{Area}(\mathcal{B}_R). \quad (\text{II.1.2})$$

Consequently, $\text{Area}(\mathcal{B}_R) \leq 4\pi R^2/3$ (this is the starting point in [CM2]). We will generalize this argument below to get area bounds for embedded disks with bounded curvature and later for more general stable domains.

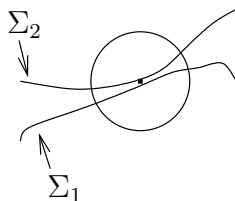


FIGURE 24. Two sufficiently close disjoint minimal surfaces with bounded curvatures must each be nearly stable.

Nearby disjoint surfaces with $|A|^2 \leq 4$ are nearly stable. See fig. 24. Recall that the Jacobi equation $Lu = \Delta u + |A|^2 u$ is the linearization of the minimal graph equation. A domain $\Omega \subset \Sigma$ is said to be stable if $\int \phi L\phi \leq 0$ for every ϕ with compact support in Ω ; i.e., if the stability inequality $\int |A|^2 \phi^2 \leq \int |\nabla \phi|^2$ holds. We will say that Ω is 1/2-stable if we have the weaker 1/2-stability inequality

$$\int |A|^2 \phi^2 \leq 2 \int |\nabla \phi|^2. \quad (\text{II.1.3})$$

One useful criterion for stability is that if $u > 0$ and $Lu = 0$ on Ω , then Ω is stable; similarly, when $u > 0$ and Lu/u is small, then Ω is 1/2-stable (cf. section 2 of [CM4]).

Roughly, if two disjoint minimal disks with $|A|^2 \leq 4$ come close at a point, then one can be written as a graph over the other of a function $u > 0$ with $Lu/u \approx 0$ and, consequently, each is 1/2-stable. This is similar to the case of geodesics. See lemmas 2.6 and 2.11 of [CM4] for the precise statements.

Area bounds when $|A|^2 \leq 4$. We first decompose an embedded minimal surface with $|A|^2 \leq 4$ into a portion with bounded area and a union of disjoint 1/2-stable domains and in the process construct a cutoff function χ which will be used in the 1/2-stability inequality:

Lemma II.1.4. (Lemma 2.15 in [CM4]). There exists C_1 so: If $0 \in \Sigma \subset B_{2R}$, $\partial\Sigma \subset \partial B_{2R}$, and $|A|^2 \leq 4$, then there exist disjoint $1/2$ -stable subdomains $\Omega_j \subset \Sigma$ and a function $\chi \leq 1$ which vanishes on $B_R \cap \Sigma \setminus \cup_j \Omega_j$ so that

$$\text{Area}(\{x \in B_R \cap \Sigma \mid \chi(x) < 1\}) \leq C_1 R^3, \quad (\text{II.1.5})$$

$$\int_{\mathcal{B}_R} |\nabla \chi|^2 \leq C_1 R^3. \quad (\text{II.1.6})$$

Proof. (Sketch). Fix $\rho > 0$ small. Given $x \in \Sigma$, let Σ_x be the component of $B_\rho(x) \cap \Sigma$ with $x \in \Sigma_x$ and let B_x^+ be the component of $B_\rho(x) \setminus \Sigma_x$ which $\mathbf{n}(x)$ points into. Set, see fig. 25,

$$VB = \{x \in B_R \cap \Sigma \mid B_x^+ \cap \Sigma \setminus \overline{\mathcal{B}_{4\rho}(x)} = \emptyset\} \quad (\text{II.1.7})$$

and let $\{\Omega_j\}$ be the components of $B_R \cap \Sigma \setminus \overline{VB}$. It follows that each Ω_j is $1/2$ -stable. Moreover, using that the points in VB are isolated, a simple ball counting argument in B_R gives (II.1.5) and (II.1.6). \square

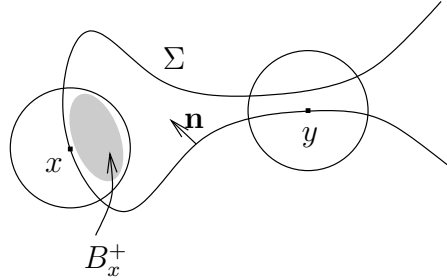


FIGURE 25. The set VB in (II.1.7):
 $x \in VB$ and $y \in \Sigma \setminus VB$.

Using the decomposition from Lemma II.1.4 in (II.1.1) (as in (II.1.2)) gives area bounds for intrinsic balls (Lemma 3.1 in [CM4]): If $0 \in \Sigma \subset B_{2R}$, $\partial\Sigma \subset \partial B_{2R}$, and $|A|^2 \leq 4$ $|A|^2(0) = 4$, then

$$\int_0^R \int_0^t \int_{\mathcal{B}_s} |A|^2 ds dt = 2(\text{Area}(\mathcal{B}_R) - \pi R^2) \leq 6\pi R^2 + 20 C_1 R^5. \quad (\text{II.1.8})$$

To see (II.1.8), let C_1 , χ , and $\cup_j \Omega_j$ be from Lemma II.1.4, so $\chi(R-r)$ vanishes off of $\cup_j \Omega_j$. Using $\chi(R-r)$ in (II.1.3), the absorbing inequality and (II.1.6) give

$$\begin{aligned} \int |A|^2 \chi^2 (R-r)^2 &\leq 2 \int (\chi^2 + 2\chi R |\nabla \chi| + R^2 |\nabla \chi|^2) \\ &\leq 6 R^2 \int_{\mathcal{B}_R} |\nabla \chi|^2 + 3 \int \chi^2 \leq 6 C_1 R^5 + 3 \text{Area}(\mathcal{B}_R). \end{aligned} \quad (\text{II.1.9})$$

We see (II.1.8) by using (II.1.5) and $|A|^2 \leq 4$ and substituting this in (II.1.1) to get

$$4(\text{Area}(\mathcal{B}_R) - \pi R^2) = \int |A|^2 (R-r)^2 \leq 10 C_1 R^5 + 3 \text{Area}(\mathcal{B}_R). \quad (\text{II.1.10})$$

Using (II.1.1) and (II.1.8), we can find large intrinsic balls with a fixed doubling:

Corollary II.1.11. (Corollary 3.5 in [CM4]). There exists C_2 so that given $\beta, R_0 > 1$, we get R so: If $0 \in \Sigma \subset B_R$ is an embedded minimal disk, $\partial\Sigma \subset \partial B_R$, $|A|^2(0) = 1$, and $|A|^2 \leq 4$, then there exists $R_0 < s < R/(2\beta)$ with

$$\int_{\mathcal{B}_{3s}} |A|^2 + \beta^{-10} \int_{\mathcal{B}_{2\beta s}} |A|^2 \leq C_2 s^{-2} \text{Area}(\mathcal{B}_s). \quad (\text{II.1.12})$$

Pointwise estimates for disks with bounded total curvature. The following curvature estimate for embedded minimal disks Σ generalizes a result of Schoen and Simon:

Proposition II.1.13. (Corollary 1.18 in [CM4]). If $\int_{\mathcal{B}_{2s}} |A|^2 \leq C_I$, then $\sup_{\mathcal{B}_s} |A|^2 \leq C_P s^{-2}$ where $C_P = C_P(C_I)$.

By (II.1.1), bounds on $\text{Area}(\mathcal{B}_t)/t^2$, $\text{Length}(\partial\mathcal{B}_t)/t$, or $\int_{\mathcal{B}_t} |A|^2$ are equivalent (if we are willing to go to subballs). Therefore, Proposition II.1.13 applies when any one of these three quantities is bounded. It is important that Σ is an embedded disk; e.g., the catenoid is complete, has finite total curvature, and is not flat.

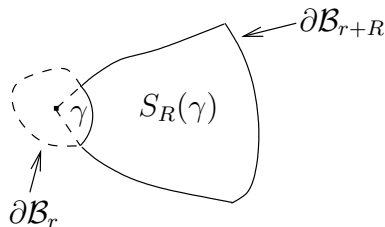


FIGURE 26. An intrinsic sector over a curve γ .

Area and total curvature of stable sectors. Given $\gamma \subset \partial\mathcal{B}_s$, define the intrinsic (truncated) sector, see fig. 26,

$$S = S_R(\gamma) = \{\exp_0(v) \mid s \leq |v| \leq s + R \text{ and } \exp_0(sv/|v|) \in \gamma\}. \quad (\text{II.1.14})$$

(Here $\exp_0 : \mathbf{R}^2 \rightarrow \Sigma$ is the exponential map at 0.) In lemma II.1.1 of [CM3], we argue as in (II.1.8) to bound the area of a stable sector S and then, using a different choice of cutoff in the stability inequality, get a total curvature bound on a subsector. New terms arise since we must cutoff along γ and along the sides of S in the stability inequality. The next lemma is an easy consequence of lemma II.1.1 and remark II.1.32 in [CM3] (k_g is the geodesic curvature of the curve γ).

Lemma II.1.15. [CM3]. Suppose that S is 1/2-stable, $\int_\gamma (1 + |k_g| s) \leq C_0 m s$, $R > 2s$, and for $x \in S$ we have $\sup_{\mathcal{B}_{s/4}(x)} |A|^2 \leq C_0 s^{-2}$. Then for $\Omega > 2$ and $2s \leq t \leq 3R/4$

$$\int_{S_{R/\Omega} \setminus \mathcal{B}_{\Omega s}} |A|^2 \leq C_1 R/s + C_2 m / \log \Omega, \quad (\text{II.1.16})$$

$$t \int_\gamma k_g \leq \text{Length}(\partial\mathcal{B}_t \cap S) \leq C_3 (m + R/s) t. \quad (\text{II.1.17})$$

Proof. (Sketch). First, argue as in (II.1.8) to get (II.1.17); the R/s term in (II.1.17) comes from the cutoff on the sides. Once we have this quadratic area growth, we then use a logarithmic cutoff in the radial direction to get (II.1.16). \square

In practice, the bound $\sup_{\mathcal{B}_{s/4}(x)} |A|^2 \leq C_0 s^{-2}$ on S in Lemma II.1.15 will be given to us by starting with a slightly larger 1/2-stable sector and then coming in from the boundary (using a comparison theorem to guarantee that the required intrinsic balls are contained in the larger sector).

Small total curvature of stable subsectors. Given a 1/2-stable sector S as in Lemma II.1.15 over a long curve γ , we can subdivide γ into subcurves so that one of the sectors over these subcurves has small total curvature. To see this, suppose that $\text{Length}(\gamma) \approx m s$ for some m large. If $m/\log \Omega$ is larger than R/s , then (II.1.16) says that the truncated sector has small average curvature $\int_{S_{R/\Omega} \setminus \mathcal{B}_{\Omega s}} |A|^2 \leq C m/\log \Omega$. If we now subdivide γ , it follows that a subsector has small total curvature.

The N -valued graph. Let S be as in Lemma II.1.15 and \hat{S} a subsector with small total curvature $\int_{\hat{S}_1} |A|^2 \leq \epsilon$ (ϵ can be made small by taking Ω , m large). It follows that $|A|^2 \leq C \epsilon r^{-2}$ on \hat{S} . Suppose that x is on the inner boundary of \hat{S} and $\gamma_x \subset \Sigma$ is the geodesic leaving x orthogonally to $\partial \hat{S}$. Integrating the curvature bound implies that, as a curve in \mathbf{R}^3 , γ_x has small total geodesic curvature and is close to a line segment. Similarly, the unit normal \mathbf{n} to Σ has small oscillation along γ_x . As we vary x , the geodesics γ_x trace out the N -valued graph Σ_g .

The proof of Theorem II.0.13: After rescaling by C/r_0 , we can assume that $\sup_{\mathcal{B}_C \cap \Sigma} |A|^2 \leq 4|A|^2(0) = 4$. The key for proving Theorem II.0.13 is to find many large intrinsic sectors with a quadratic curvature bound. To do this, we first use Proposition II.1.13 to bound $\text{Length}(\partial \mathcal{B}_R)/R$ from below for $R \geq R_0$. Corollary II.1.11 gives $R_3 > R_0$ and many long disjoint curves $\tilde{\gamma}_i \subset \partial \mathcal{B}_{R_3}$ so the sectors over $\tilde{\gamma}_i$ have bounded $\int |A|^2$. Proposition II.1.13 gives the pointwise curvature bound. Once we have these sectors, two must be close and, hence, also 1/2-stable. Lemma II.1.15 gives a subsector with small total curvature which then must contain the N -valued graph Σ_g (this is done in corollary II.1.34 of [CM3]).

II.2. THE ESTIMATE BETWEEN THE SHEETS AND THE EXTENSION

In this section, we will give an overview of the proof of Theorem II.0.15 where we extend the multi-valued graphs almost to the boundary. This result is significantly more subtle than the local existence result discussed in the previous section. We only give a very rough outline of the proof and refer to [CM3] for the full story.

The key component of the proof of the extension theorem is a curvature estimate “between the sheets” for embedded minimal disks in \mathbf{R}^3 . We will think of an axis (see fig. 28) for such a disk Σ as a point or curve away from which the surface locally (in an extrinsic ball) has more than one component. With this weak notion of an axis, our estimate is that if one component of Σ is sandwiched between two others that connect to an axis, then the one that is sandwiched has curvature estimates; see Theorem II.2.1. The example to keep in mind is a helicoid and the components are “consecutive sheets” away from the axis.

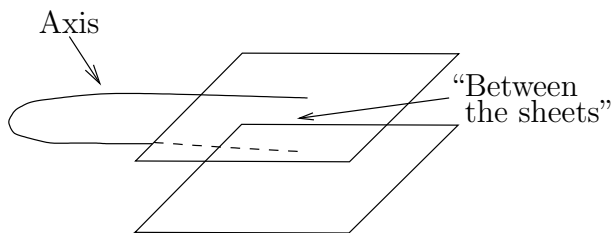


FIGURE 27. The estimate between the sheets; Theorem II.2.1.

Let $\gamma_{p,q}$ denote the line segment from p to q and $T_s(\gamma_{p,q})$ its s -tubular neighborhood. A curve γ is h -almost monotone if given $y \in \gamma$, then $B_{4h}(y) \cap \gamma$ has only one component which intersects $B_{2h}(y)$. Our curvature estimate “between the sheets” is:

Theorem II.2.1. (Theorem I.0.8 in [CM3]). See fig. 28. There exist $c_1 \geq 4$, $2c_2 < c_4 < c_3 \leq 1$ so: Let $\Sigma \subset B_{c_1 r_0}$ be an embedded minimal disk with $\partial\Sigma \subset \partial B_{c_1 r_0}$ and $y \in \partial B_{2r_0}$. Suppose $\Sigma_1, \Sigma_2, \Sigma_3$ are distinct components of $B_{r_0}(y) \cap \Sigma$ and $\gamma \subset (B_{r_0} \cup T_{c_2 r_0}(\gamma_{0,y})) \cap \Sigma$ is a curve with $\partial\gamma = \{y_1, y_2\}$ where $y_i \in B_{c_2 r_0}(y) \cap \Sigma_i$ and each component of $\gamma \setminus B_{r_0}$ is $c_2 r_0$ -almost monotone. Then any component Σ'_3 of $B_{c_3 r_0}(y) \cap \Sigma_3$ with y_1, y_2 in distinct components of $B_{c_4 r_0}(y) \setminus \Sigma'_3$ is a graph.

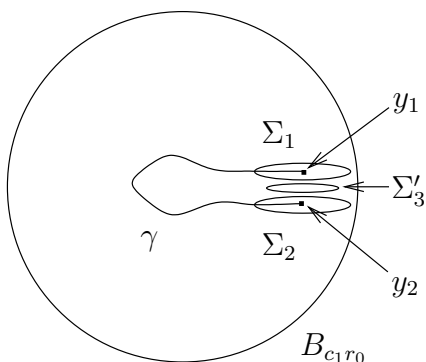


FIGURE 28. $y_1, y_2, \Sigma_1, \Sigma_2, \Sigma'_3$, and γ in Theorem II.2.1.

The idea of the proof of Theorem II.2.1 is to show that if this were not the case, then we could find an embedded stable disk that would be almost flat and lie in the complement of the original disk. In fact, we can choose the stable disk to be sandwiched between the two components as well. The flatness would force the stable disk to eventually cross the axis in the original disk, contradicting that they were disjoint.

The curve γ in Theorem II.2.1 which plays the role of an axis and connects Σ_1 and Σ_2 can in many instances be extended using the maximum principle once it occurs on a given small scale; cf. lemma I.0.11 of [CM3]. This is used both in the proof of Theorem II.2.1 and in the applications of it.

Overview of the proof of Theorem II.0.15: The first step (part I of [CM3]) is to show Theorem II.2.1 when the surface is in a slab; i.e., when $\Sigma \subset \{|x_3| \leq \beta h\}$.

The second step (part II of [CM3]) is to show that certain stable disks starting off as multi-valued graphs remain the same. This is needed when we generalize the results of step one to when the surface is not anymore in a slab.

Two facts go into the proof of the extension of stable disks. First, we show that if an almost flat multi-valued graph sits inside a stable disk, then the outwardly defined intrinsic sector from a curve which is a multi-valued graph over a circle has a subsector which is almost flat; cf. Lemma II.1.15 and the paragraph “Small total curvature of stable subsectors” above. As the initial multi-valued graph becomes flatter and the number of sheets in it goes up, the subsector becomes flatter. The second fact is that the separation between the sheets grows sublinearly; (I.1.1).

The first application of these two facts is to extend the middle sheet as a multi-valued graph. This is done by dividing the initial multi-valued graph (or curve in the graph that is itself a multi-valued graph over the circle) into three parts where the middle sheet is the second part. The idea is then that the first and third parts have subsectors which are almost flat multi-valued graphs and the middle part (which has curvature estimates since it is stable) is sandwiched between the two others. Hence its sector is also almost flat.

A thing that adds some technical complications to the above picture is that in the result about almost flat subsectors it is important that the ratio between the size of the initial multi-valued graph and how far one can go out is fixed. This is because the estimate for the subsector comes from a total curvature estimate which is in terms of this ratio (see (II.1.16)) and can only be made small by looking at a fixed large number of rotations for the graph. This forces us to successively extend the multi-valued graph. The issue is then to make sure that as we move out in the sector and repeat the argument we have essentially not lost sheets. This is taken care of by using the sublinear growth of the separation between the sheets together with the Harnack inequality and the maximum principle. (The maximum principle is used to make sure that as we try to recover sheets after we have moved out then we don't hit the boundary of the disk before we have recovered essentially all of the sheets that we started with.) The last thing which is used is theorem 3.36 in [CM10]. This is used to guarantee that, as we patch together these multi-valued graphs coming from different scales, then the surface that we get is still a multi-valued graph over a fixed plane.

The third step (part III of [CM3]) is to generalize the curvature estimate between the sheets to the case where the surface is not anymore in a slab. This uses the extension of the stable graphs from step two.

Finally, using steps one, two, and three we showed Theorem II.0.15 in part IV of [CM3].

Part III. The proof of the one-sided curvature estimate

In appendix A of [CM6] we showed curvature estimates for minimal hyper-surfaces in \mathbf{R}^n which on all sufficiently small scales lie on one side of, but come close to, a hyper-plane. Such a scale invariant version of Theorem I.3.2 can (unlike Theorem I.3.2) be proven quite easily by a blow up argument using the minimal surface equation. Moreover, such a scale invariant condition is very similar to the classical Reifenberg property. (After all, a subset of \mathbf{R}^n has the Reifenberg property if it is close on all scales to a hyper-plane.) As explained in Part I (in particular Corollary I.3.7), the significance of Theorem I.3.2 is indeed that it only requires closeness on one scale. On the other hand, this is what makes it difficult to

prove and requires us to use the results discussed in the previous parts together with results from [CM5].

Let us briefly outline the proof of the one-sided; i.e., Theorem I.3.2. Suppose that Σ is an embedded minimal disk in the half-space $\{x_3 > 0\}$. We prove the curvature estimate by contradiction; so suppose that Σ has low points with large curvature. Starting at such a point, we decompose Σ into disjoint multi-valued graphs using the existence of nearby points with large curvature given by corollary III.3.5 of [CM5], a blow up argument, and [CM3], [CM4]. The key point is then to show (see Proposition III.0.2 below) that we can in fact find such a decomposition where the “next” multi-valued graph starts off a definite amount below where the previous multi-valued graph started off. In fact, what we show is that this definite amount is a fixed fraction of the distance between where the two graphs started off. Iterating this eventually forces Σ to have points where $x_3 < 0$. This is the desired contradiction.

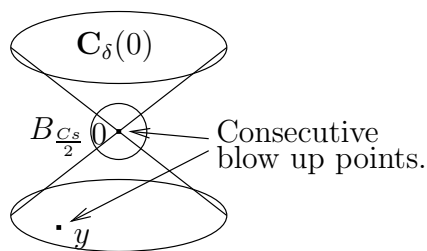


FIGURE 29. Proposition III.0.2: Two consecutive blow up points satisfying (III.0.4).

Proposition III.0.2. (See proposition III.2.2 in [CM6] for the precise statement). See fig. 29. There exists $\delta > 0$ such that if $(0, s)$ satisfies (III.0.4) and $\Sigma_0 \subset \Sigma$ is the corresponding (to $(0, s)$) 2-valued graph over $D_R \setminus D_s$, then we get (y, t) satisfying (III.0.4) with $y \in C_\delta(0) \cap \Sigma \setminus B_{C_s/2}$ and where y is below Σ_0 .

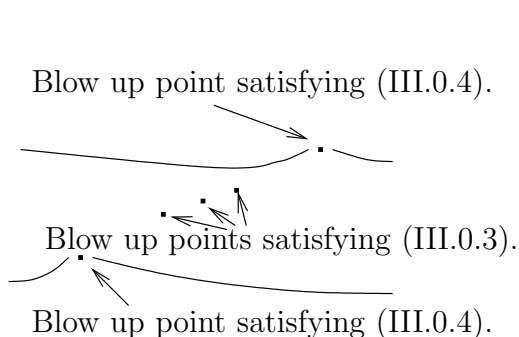


FIGURE 30. Between two consecutive blow up points satisfying (III.0.4) there are a bunch of blow up points satisfying (III.0.3).

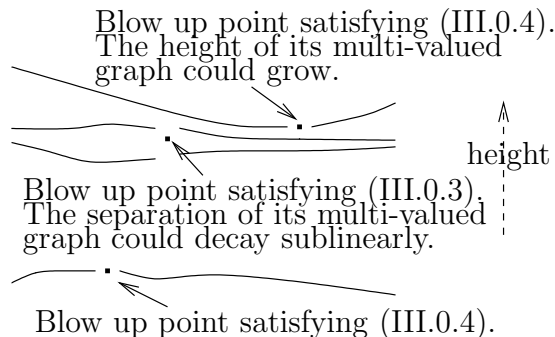


FIGURE 31. Measuring height. Blow up points and corresponding multi-valued graphs.

To prove this key proposition (Proposition III.0.2), we use two decompositions and two kinds of blow up points. The first decomposition uses the more standard blow up points

given as pairs (y, s) where $y \in \Sigma$ and $s > 0$ is such that

$$\sup_{\mathcal{B}_{8s}(y)} |A|^2 \leq 4|A|^2(y) = 4C_1^2 s^{-2}. \quad (\text{III.0.3})$$

The point about such a pair (y, s) is that by [CM3], [CM4] (and an argument in section II.2 of [CM6] which allows us replace extrinsic balls by intrinsic ones), then Σ contains a multi-valued graph near y starting off on the scale s . (This is assuming that C_1 is a sufficiently large constant given by [CM3], [CM4].) The second kind of blow up points are the ones where (except for a technical issue) 8 is replaced by some really large constant C , i.e.,

$$\sup_{\mathcal{B}_{Cs}(y)} |A|^2 \leq 4|A|^2(y) = 4C_1^2 s^{-2}. \quad (\text{III.0.4})$$

The point will then be that we can find blow up points satisfying (III.0.4) so that the distance between them is proportional to the sum of the scales. Moreover, between consecutive blow up points satisfying (III.0.4), we can find a bunch of blow up points satisfying (III.0.3); see fig. 30. The advantage is now that if we look between blow up points satisfying (III.0.4), then the height of the multi-valued graph given by such a pair grows like a small power of the distance whereas the separation between the sheets in a multi-valued graph given by (III.0.3) decays like a small power of the distance; see fig. 31. Now thanks to that the number of blow up points satisfying (III.0.3) (between two consecutive blow up points satisfying (III.0.4)) grows almost linearly then, even though the height of the graph coming from the blow up point satisfying (III.0.4) could move up (and thus work against us), then the sum of the separations of the graphs coming from the points satisfying (III.0.3) dominates the other term. Thus the next blow up point satisfying (III.0.4) (which lies below all the other graphs) is forced to be a definite amount lower than the previous blow up point satisfying (III.0.4).

Part IV. The local case

Consider a sequence of (compact) embedded minimal disks $\Sigma_i \subset B_{R_i} = B_{R_i}(0) \subset \mathbf{R}^3$ with $\partial\Sigma_i \subset \partial B_{R_i}$ and either:

- (a) R_i equal to a finite constant.
- (b) $R_i \rightarrow \infty$.

Case (a) is what we call the *local case* and (b) is what we refer to as the *global case*; Theorem I.0.4 dealt with the global case. Recall also that a surface $\Sigma \subset \mathbf{R}^3$ is said to be properly embedded if it is embedded and the intersection of Σ with any compact subset of \mathbf{R}^3 is compact. We say that a lamination or foliation is proper if each leaf is proper.

We are interested in the possible limits of sequences of minimal disks Σ_i as above where the curvatures blow up, e.g., $\sup_{B_1 \cap \Sigma_i} |A|^2 \rightarrow \infty$ as $i \rightarrow \infty$. In the global case, Theorem I.0.4 gave a subsequence converging off of a Lipschitz curve to a foliation by parallel planes. In particular, the limit is a (smooth) foliation which is proper. We showed in [CM16] (see Theorem IV.0.5 below) that smoothness and properness of the limit can fail in the local case; cf. fig. 32.

Namely, Theorem IV.0.5, constructs a sequence of disks $\Sigma_i \subset B_1$ as above where the curvatures blow up only at 0 and $\Sigma_i \setminus \{x_3\text{-axis}\}$ consists of two multi-valued graphs for each i ; see (1), (2), and (3). Furthermore (see (4)), $\Sigma_i \setminus \{x_3 = 0\}$ converges to two embedded minimal disks $\Sigma^- \subset \{x_3 < 0\}$ and $\Sigma^+ \subset \{x_3 > 0\}$ each of which spirals into $\{x_3 = 0\}$ and thus is not proper; see fig. 32.

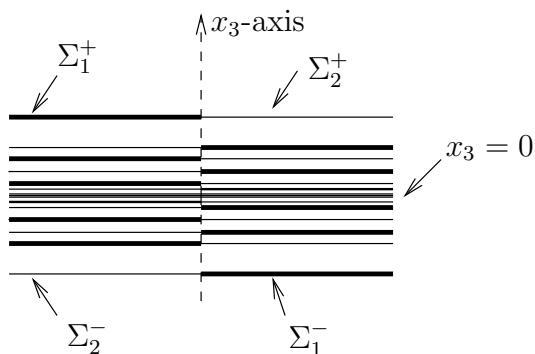


FIGURE 32. A schematic picture of the limit in Theorem IV.0.5 which is not smooth and not proper (the dotted x_3 -axis is part of the limit). The limit contains four multi-valued graphs joined at the x_3 -axis; Σ_1^+ , Σ_2^+ above the plane $x_3 = 0$ and Σ_1^- , Σ_2^- below the plane. Each of the four spirals into the plane.

Theorem IV.0.5. (Theorem 1 in [CM16]). See fig. 32. There is a sequence of compact embedded minimal disks $0 \in \Sigma_i \subset B_1 \subset \mathbf{R}^3$ with $\partial\Sigma_i \subset \partial B_1$ and containing the vertical segment $\{(0, 0, t) \mid |t| < 1\} \subset \Sigma_i$ so:

- (1) $\lim_{i \rightarrow \infty} |A_{\Sigma_i}|^2(0) = \infty$.
- (2) $\sup_i \sup_{\Sigma_i \setminus B_\delta} |A_{\Sigma_i}|^2 < \infty$ for all $\delta > 0$.
- (3) $\Sigma_i \setminus \{x_3\text{-axis}\} = \Sigma_{1,i} \cup \Sigma_{2,i}$ for multi-valued graphs $\Sigma_{1,i}$ and $\Sigma_{2,i}$
- (4) $\Sigma_i \setminus \{x_3 = 0\}$ converges to two embedded minimal disks $\Sigma^\pm \subset \{\pm x_3 > 0\}$ with $\overline{\Sigma^\pm} \setminus \Sigma^\pm = B_1 \cap \{x_3 = 0\}$. Moreover, $\Sigma^\pm \setminus \{x_3\text{-axis}\} = \Sigma_1^\pm \cup \Sigma_2^\pm$ for multi-valued graphs Σ_1^\pm and Σ_2^\pm which spiral into $\{x_3 = 0\}$; see fig. 32.

It follows from (4) that $\Sigma_i \setminus \{0\}$ converges to a lamination of $B_1 \setminus \{0\}$ (with leaves Σ^- , Σ^+ , and $B_1 \cap \{x_3 = 0\} \setminus \{0\}$) which does not extend to a lamination of B_1 . Namely, 0 is not a removable singularity.

REFERENCES

- [ChC] J. Cheeger and T. H. Colding, On the Structure of Spaces with Ricci Curvature Bounded Below; I, *Jour. of Diff. Geometry* 46 (1997) 406-480.
- [CM1] T.H. Colding and W.P. Minicozzi II, Minimal surfaces, Courant Lecture Notes in Math., v. 4, 1999.
- [CM2] T.H. Colding and W.P. Minicozzi II, Estimates for parametric elliptic integrands, *International Mathematics Research Notices*, no. 6 (2002) 291-297.
- [CM3] T.H. Colding and W.P. Minicozzi II, The space of embedded minimal surfaces of fixed genus in a 3-manifold I; Estimates off the axis for disks, preprint (2001). math.AP/0210106.
- [CM4] T.H. Colding and W.P. Minicozzi II, The space of embedded minimal surfaces of fixed genus in a 3-manifold II; Multi-valued graphs in disks, preprint (2001). math.AP/0210086.
- [CM5] T.H. Colding and W.P. Minicozzi II, The space of embedded minimal surfaces of fixed genus in a 3-manifold III; Planar domains, preprint. math.AP/0210141.
- [CM6] T.H. Colding and W.P. Minicozzi II, The space of embedded minimal surfaces of fixed genus in a 3-manifold IV; Locally simply connected, preprint. math.AP/0210119.

- [CM7] T.H. Colding and W.P. Minicozzi II, The space of embedded minimal surfaces of fixed genus in a 3-manifold V; Fixed genus, in preparation.
- [CM8] T.H. Colding and W.P. Minicozzi II, Multi-valued minimal graphs and properness of disks, *International Mathematics Research Notices*, no. 21 (2002) 1111-1127.
- [CM9] T.H. Colding and W.P. Minicozzi II, On the structure of embedded minimal annuli, *International Mathematics Research Notices*, no. 29 (2002) 1539-1552.
- [CM10] T.H. Colding and W.P. Minicozzi II, Minimal annuli with and without slits, *Jour. of Symplectic Geometry*, vol. 1, issue 1 (2002) 47-62.
- [CM11] T.H. Colding and W.P. Minicozzi II, Complete properly embedded minimal surfaces in \mathbf{R}^3 , *Duke Math. J.* 107 (2001), no. 2, 421-426.
- [CM12] T.H. Colding and W.P. Minicozzi II, Convergence of embedded minimal surfaces without area bounds in three manifolds, *C.R. Acad. Sci. Paris* t. 327, Série I (1998) 765-770.
- [CM13] T.H. Colding and W.P. Minicozzi II, Removable singularities for minimal limit laminations, *C.R. Acad. Sci. Paris* t. 331, Série I (2000) 465-468.
- [CM14] T.H. Colding and W.P. Minicozzi II, Embedded minimal surfaces without area bounds in 3-manifolds. Geometry and topology: Aarhus (1998), 107-120, *Contemp. Math.*, 258, Amer. Math. Soc., Providence, RI, 2000.
- [CM15] T.H. Colding and W.P. Minicozzi II, Disks that are double spiral staircases, preprint 2002. math.AP/0208181.
- [CM16] T.H. Colding and W.P. Minicozzi II, Embedded minimal disks: Proper versus nonproper - global versus local, preprint 2002. math.DG/0210328.
- [MeRo] W. Meeks III and H. Rosenberg, The uniqueness of the helicoid and the asymptotic geometry of properly embedded minimal surfaces with finite topology, preprint.

COURANT INSTITUTE OF MATHEMATICAL SCIENCES AND PRINCETON UNIVERSITY, 251 MERCER STREET,
NEW YORK, NY 10012 AND FINE HALL, WASHINGTON RD., PRINCETON, NJ 08544-1000

DEPARTMENT OF MATHEMATICS, JOHNS HOPKINS UNIVERSITY, 3400 N. CHARLES ST., BALTIMORE,
MD 21218

E-mail address: colding@cims.nyu.edu, minicozz@jhu.edu